Clean Manuscript

TITTLE PAGE

Paeonol attenuates LPS-induced endothelial dysfunction and apoptosis by inhibiting BMP4 and TLR4 signalling simultaneously but independently

Ker Woon Choy, Yeh Siang Lau, Dharmani Murugan, Paul M. Vanhoutte, Mohd Rais Mustafa

Department of Pharmacology, Faculty of Medicine, University of Malaya, Kuala Lumpur, Malaysia (KWC, YSL, DM, MRM).

State Key Laboratory of Pharmaceutical Biotechnology, Department of Pharmacology and Pharmacy, Li Ka Shing Faculty of Medicine, The University of Hong Kong, Hong Kong (PMV).

RUNNING TITLE PAGE

a) Running Tittle: Paeonol attenuates LPS-induced endothelial dysfunction

b) Correspondence author:

Name: Mohd Rais Mustafa

Address: Department of Pharmacology, University of Malaya, Kuala Lumpur 50603, Malaysia.

E-mail: rais@um.edu.my

Phone number: +603-7967 4702

c) The number of text pages: 35

Number of tables: 1 (Supplementary)

Number of figures: 9 figures, 5 supplemental figures, 1 visual abstract

Number of references: 46

Number of words in the Abstract: 246

Number of words in the Introduction: 658

Number of words in the Discussion: 947

d) Abbreviations:

AG, Aminoguanidine; ALK3, activing receptor-like kinase 3; AMPK, 5' adenosine monophosphate-activated protein kinase; ANOVA, one-way analysis of variance; BMP4, bone morphogenic protein 4; BMPER, bone morphogenetic protein-binding endothelial regulator; BMPR1A, BMP receptor type 1A; BSA, Bovine serum albumin DETCA, Diethylthiocarbamic acid; DHE, dihydroethidium fluorescence; DMEM, Dulbecco's Modified Eagle Medium; DPI, Diphenylene iodonium; ECL, enhanced chemiluminescence; ECM, endothelial cell medium; eNOS, endothelial nitric oxide

synthase; ER, endoplasmic reticulum; H_2O_2, hydrogen peroxide; HUVECs, human umbilical vein endothelial cells; iNOS, inducible nitric oxide synthase; LPS, lipopolysaccharides; MAPK, mitogen-activated protein kinases; NADPH, nicotinamide adenine dinucleotide phosphateoxidase; NFκB, nuclear factor κB; NO, Nitric oxide; NOX2, nicotinamide adenine dinucleotide phosphate oxidase subunit 2; NPSS, normal physiological solution; PBS, phosphate buffered saline; PI, propidium iodide; PPARδ, peroxisome proliferator-activated receptor δ; RIPA, radioimmunoprecipitation assay; ROS, reactive oxygen species; TGF-β, transforming growth factors-β; TLR4, toll like receptor 4.

e) Section assignment: Cardiovascular

Abstract

Inflammatory injury of the endothelium leads to apoptosis and endothelial dysfunction. The current study explored the effect and mechanisms of paeonol in inflammation-induced apoptosis and endothelial dysfunction induced by lipopolysaccharides (LPS). The effects of paeonol on LPS-induced inflammatory injury were assessed by Western blotting, flow cytometry and reactive oxygen species (ROS) measurement in human umbilical vein endothelial cells (HUVECs) and C57BL/6J mice. Vascular reactivity of isolated mouse aortae was examined using wire myographs. Exposure of HUVECs to LPS increased the protein presence of toll like receptor 4 (TLR4), bone morphogenic protein 4 (BMP4), BMP receptor type 1A (BMPR1A), nicotinamide adenine dinucleotide phosphate oxidase subunit 2 (NOX2), mitogen-activated protein kinases (MAPK), inducible nitric oxide synthase (iNOS) and cleaved caspase 3 as well as decreased in phosphorylated endothelial nitric oxide synthase (eNOS); these effects were prevented by treatment with paeonol. Similarly, co-treatment with paeonol reversed BMP4-induced apoptosis in HUVECs. Relaxations to the endothelium-dependent vasodilator acetylcholine were impaired in mouse aortae after exposure to LPS; this endothelial dysfunction was reversed by co-treatment with paeonol, noggin (BMP4 inhibitor), TAK242 (TLR4 antagonist), apocynin (ROS scavenger), MAPK inhibitors and aminoguanidine (iNOS inhibitor). BMP4 siRNAs abolished LPS-induced upregulation of BMP4 and cleaved caspase 3 protein but not in cells treated with TLR4 siRNA, and *vice versa*. Silencing of TLR4 and BMP4 abolished the inhibitory effects of paeonol on LPS-induced activation of cleaved caspase 3. The present results demonstrate that paeonol reduces LPS-induced endothelial dysfunction and apoptosis by inhibiting TLR4 and BMP4 signalling independently.

Introduction

Paeonol (Figure 1) isolated from Moutan cortex, root bark of the *Paeonia suffruticosa* Andrews plant (Lau et al., 2007) possess anti-atherosclerosis, anti-inflammatory, anti-oxidant, anti-diabetic and anti-tumor properties (Lau et al., 2007; Sun et al., 2008; Li et al., 2009). The phytoactive compound prevents lung inflammation and fibrosis induced by bleomycin in mice and rats (Meng-Han Liu, 2014) and lipopolysaccharide (LPS) (Li et al., 2012). *In vitro* and *in vivo*, paeonol also decreases inflammation and injury induced by LPS in N9 microglia cells and in murine kidneys by inhibiting the toll like receptor 4 (TLR4) and nuclear factor κB (NFκB) signalling pathways (Tseng et al., 2012; Fan et al., 2016). Additionally, paeonol suppresses cigarette smoke-induced release of interleukin-8 by virtue of its anti-oxidant properties and by inhibiting both reactive oxygen species (ROS)-sensitive 5' adenosine monophosphate-activated protein kinase (AMPK)/ mitogen-activated protein kinases (MAPK) signalling and the downstream NF-κB, thus reducing pulmonary inflammation (Meng-Han Liu, 2014). In the rat, the combination of paeonol with *Danshensuin* exerts cardioprotective effects on isoproterenol-induced myocardial injury (Li et al., 2012). Furthermore, paeonol protects against endoplasmic reticulum (ER)-stress induced endothelial dysfunction by enrolling AMPK and peroxisome proliferator-activated receptor δ (PPARδ) signalling pathways (Choy et al., 2016) and by inhibiting oxidative stress (Choy et al., 2017). Chronic supplementation with paeonol combined with *Danshensu* improves vascular reactivity in the basilar artery of diabetic rats by reducing oxidative stress and the intracellular Ca^{2+}-concentration (Hu et al., 2012). In addition, paeonol has a direct vasodilator effect which is attributed to inhibition of voltage-dependent and receptor-operated Ca^{2+} channels, as well as to inhibition of intracellular Ca^{2+} release (Li et al., 2010).

Lipopolysaccharides (LPS), a major constituent of bacterial outer membranes, play an important role in the initiation of inflammation and microvascular leaking (Mann et al., 2010). LPS can bind to toll-like receptor 4 (TLR4), and disrupt the endothelial barrier by activating intracellular signalling pathways that stimulate alteration of the cytoskeletal architecture of the endothelial cells (Bannerman and Goldblum, 1999; Cuschleri et al., 2003). LPS induces apoptosis and detachment of endothelial cells, an event which contributes to the pathogenesis of sepsis and its attendant complications [disseminated intravascular coagulation, systemic vascular collapse, multiorgan failure, development of vascular leaks, and acute respiratory distress (Bannerman and Goldblum, 2003)]. Bone morphogenic protein 4 (BMP4), a member of the transforming growth factors-β (TGF-β) superfamily, was originally discovered to play an important role in cartilage formation, bone mineralization, and early embryonic development (Chen et al., 2004). BMP4 is upregulated in the lung during LPS-induced inflammation, and in airway epithelial cells treated with either LPS or tumor necrosis factor-alpha (TNF-α) (Li et al., 2014). Furthermore, BMPER (bone morphogenetic protein-binding endothelial regulator), an extracellular modulator of bone morphogenetic protein signalling has been identified as a vital component that regulates inflammatory responses in LPS-induced acute lung injury (Lockyer et al., 2017). BMP4 exerts pro-inflammatory effects resulting in enhanced leukocyte adhesion to the endothelial surface *in vitro* (Csiszar et al., 2006) and impairs endothelial function, in the mouse aorta, through accumulation of reactive oxygen species (ROS) generated by subunits (NOX1, NOX2, and NOX4) of nicotinamide adenine dinucleotide phosphate (NADPH) oxidase (Miriyala et al., 2006; Csiszar et al., 2007). In endothelial cells, BMP4 binds to BMPR1A-receptors which in turn induces endothelial cell-apoptosis mediated by the oxidative stress-dependent p38MAPK and JNK pathway (Tian et al., 2012).

Limited information is available concerning the effect of paeonol on inflammation-mediated apoptosis and endothelial dysfunction, as well how the underlying mechanism relates to the LPS/TLR4 and BMP4 signalling pathways. Therefore, the aim of the present study was to investigate, in a model of inflammation: (a) the molecular and cellular mechanisms underlying the protection exerted by paeonol against endothelial dysfunction; and (b) identify the involvement of BMP4 in LPS-induced endothelial cell apoptosis and endothelial dysfunction as a possible pharmacological target of paeonol. In particular, the present experiments tested the hypothesis that paeonol reduces both acute inflammation secondary to LPS-induced apoptosis and endothelial dysfunction by inhibiting the BMP4 signalling pathway.

Materials and Methods

Human endothelial cell culture

Human umbilical vein endothelial cells (HUVECs, ScienCell, Corte Del Cedro Carlsbad, CA, USA) were cultured in endothelial cell medium (ECM) supplemented with 5% fetal bovine serum, 1% penicillin-streptomycin and 1% endothelial cell growth supplement, maintained at 37 °C and aerated with 5% CO_2, 95% O_2. The cells (passage 4 to 6) were used when reaching 80-90% confluence. For all experiments, HUVECs were seeded and grown overnight to sub-confluence level before incubation (24 hours), in ECM, with LPS, (0.1, 0.5 and 1μg/mL), hydrogen peroxide (H_2O_2, 200 μM) and various concentrations of paeonol (0.01, 0.1 and 1 μM,) before collection for apoptosis and protein assays. For other drug treatments, HUVECs were co-treated during 24 hours with one of the following: recombinant BMP4 (100 ng/mL, dissolved in 4 mM HCl with 0.1% BSA), noggin (100 ng/mL, BMP4 antagonist), apocynin (20 μM, NADPH oxidase inhibitor), SP600125 (10 μM, JNK inhibitor), SB202190 (10 μM, p38 MAPK inhibitor), aminoguanidine (100 μM, selective inhibitor of inducible NOS) and TAK242 (1 μM, TLR4 antagonist).

Flow cytometry quantification of apoptosis

The percentage of apoptotic cells was measured using the Annexin V-FITC apoptosis assay kit according to manufacturer's instructions (BD Biosciences, San Jose, CA, USA). Briefly, HUVECs were seeded in six-well plates and were treated with various concentrations of either LPS (0.1, 0.5 and 1 μg/mL) or H_2O_2 (200 μM; serving as a positive control) together with paeonol (0.01, 0.1 and 1 μM) during 24 hours. After treatments, cells were harvested by trypsinization, washed and re-suspended in 1 mL of binding buffer (1×10^6 cells/mL). Approximately 1×10^5 cells were stained with propidium iodide (PI) and Annexin-V FITC at

room temperature during 15 minutes in the dark before analysis with a FACSort flow cytometer (BD Biosciences). Results were analysed with the Cell Quest Pro software (BD Biosciences). The amount of apoptosis was determined as the percentage of annexin V-positive cells over PI-negative cells (Bao et al., 2013).

Transient transfection with siRNA

HUVECs (2 x 10^4 per well) were seeded into six-well plates and grown overnight. The amount of siRNA was optimized following the manufacturer's instructions. The siRNA targeting TLR4 or BMP4 (ON-TARGETplus SMART pool small interferingRNA; Dharmacon, Thermo Scientific, Lafayette, CO) or scrambled siRNA (ON-TARGETplus Control Nontargeting pool; Dharmacon) were transfected into the cells using Dharmafect 1 transfection reagent (Dharmacon). Compared to unrelated control siRNAs and scrambled siRNAs, the specific siRNA-concentration resulting in more than 60% knockdown in protein levels was chosen, as determined by Western blotting. The media were refreshed, 72 hours *post* transfection with BMP4 siRNAs or 48 hours *post* transfection with TLR4 siRNAs, and the cells were incubated with vehicle, LPS (1 μg/mL) and paeonol (1 μM) during 24 hours before being harvested for Western blotting.

Animals

The experiments were performed on male mice, because they are more prone than females to LPS-induced inflammation (Everhardt Queen et al., 2016). C57BL/6J mice were supplied by Monash University (Sunway Campus, Selangor, Malaysia) and housed in well ventilated room at a constant temperature of 23 ºC with a 12 hours light/dark cycle. They were provided with normal mice chow (Specialty Feeds Pty Ltd., Glen Forrest, Australia) and tap water *ad libitum.* All of the experiments were conducted according to the Guide for the Care and Use of

Laboratory Animals as adopted and promulgated by the U.S. National Institutes of Health, and were approved by University of Malaya Animal Care and Ethics Committee (Ethics reference no: 2016-170531/PHAR/R/MRM).

Induction of inflammation and chronic treatment in mice

Twelve weeks-old mice were randomly assigned into six groups (n=6-7) of mice receiving: (a) vehicle [phosphate buffered saline, PBS, intraperitoneal injection] only (controls); (b) an intraperitoneal injection of LPS (15 mg/kg) and vehicle (saline, 100 μL by oral gavage) (LPS); (c) LPS plus oral administration of paeonol (20 mg/kg) (LPS+ paeonol); (d) oral administration of paeonol (20 mg/kg) (Paeonol); (e) LPS plus intraperitoneal injections of noggin (0.5 mg/kg/day; BMP4 antagonist) one hour before and two, four and six hours after the LPS injection (LPS + Noggin); (6) LPS plus an intraperitoneal injection of TAK242 (3 mg/kg/; TLR4 antagonist) one hour before the LPS injection (LPS + TAK242). The doses of LPS and paeonol were determined from the literature (Hsieh et al., 2006; Lee et al., 2013; Shi et al., 2016) and preliminary data (Supplemental Figure 1A&B) which showed that 20 mg/kg paeonol improved relaxations to the endothelium-dependent vasodilator acetylcholine in mice treated with LPS (15 mg/kg). The animals were humanely sacrificed by CO_2 inhalation at the end of the 24 hours of treatment.

Organ culture of isolated aortae

Aortae from C57BL/6J mouse were isolated and cultured in Dulbecco's Modified Eagle Medium (DMEM; Gibco, Gaithersburg, MD, USA) supplemented with 10% Fetal Bovine Serum (Gibco), containing 100 U/mL penicillin and 100 μg/mL streptomycin (Gibco). The rings were incubated during 24 hours in the absence or presence of LPS (1 μg/mL), paeonol (1 μM), recombinant BMP4 (100 ng/mL, dissolved in 4 mM HCl with 0.1% bovine serum

albumin), noggin (100 ng/mL), SP600125 (10 μM), SB202190 (10 μM), apocynin (20 μM), aminoguanidine (100μM), TAK242 (1 μM) and indomethacin (10 μM) in an incubator (5% CO_2; 37°C) and thereafter transferred to wire myographs for functional studies.

Functional Studies

After 24 hours, the mice were killed by CO_2 inhalation and their thoracic aortae were excised and cleaned of adjacent connective tissues and fat with extra care to avoid any damage to the endothelium. The aortae were cut into several rings (2 mm in length). The rings were suspended in a Multi-Wire Myograph System (Danish Myo Technology, Aarhus, Denmark) and bathed in oxygenated modified Krebs physiological salt solution (pH 7.4) of the following composition (in mM): NaCl 119, $NaHCO_3$ 25, KCl 4.7, KH_2PO_4 1.2, $MgSO_4.7H_2O$ 1.2, glucose 11.7 and $CaCl_2.2H_2O$ 2.5 (control solution). Some arteries were snap-frozen in liquid nitrogen and stored at -80°C for further experiments. All rings were stretched to an optimal baseline tension of 3 mN and maintained at 37 °C with continuous oxygenation with 95% O_2 and 5% CO_2 (Choy et al., 2017). After equilibration (30 minutes), the rings were contracted with 60 mM KCl and washed three times in control solution. Then, they were contracted with phenylephrine (1 μM, α-adrenergic agonist) to establish a stable tension. Cumulative concentration-response curves were obtained for both endothelium-dependent (acetylcholine, 3nM to 10 μM) and endothelium-independent (sodium nitroprusside, 1nM to 10 μM) vasodilators. Paeonol and the other pharmacological inhibitors tested did not significantly affect the contractions evoked by phenylephrine (data not shown). Changes in isometric tension were recorded with a PowerLab LabChart 6.0 recording system (AD Instruments, Bella Vista, NSW, Australia).

Western blotting

After treatment, HUVECs and aortae were homogenized and lysed in ice-cold radioimmunoprecipitation assay (RIPA) buffer containing leupeptin 1 μg/mL, aprotinin 5 μg/mL, PMSF 100 μg/mL, sodium orthovanadate 1 mM, EGTA 1 mM, EDTA 1 mM, NaF 1 mM, and β-glycerolphosphate 2 mg/mL (Sigma Aldrich; St.Louis, MO, USA) followed by centrifugation (15,000 X g during 30 minutes) at 4°C to collect supernatants for Western blotting. Protein concentrations of the supernatant were determined by a modified Lowry assay (Bio-Rad Laboratories, Hercules, CA, USA). Samples of protein (15 μg) loaded on 7.5 or 15% sodium dodecyl sulphate polyacrylamide gels and transferred to an immobilon-P polyvinylidene difluoride membrane (Millipore, Billerica, MA, USA) at 100 V. The non-specific binding was blocked with 3% bovine serum albumin in Tris-buffered saline containing 0.1% Tween-20 (TBS-T) for one hour at room temperature under gentle shaking. After washing in TBS-T, the blots were incubated with primary antibodies against phospho-p38 MAPK, p38 MAPK, phospho-SAPK/JNK, SAPK/ JNK (1:1000, Cell signaling Technology, Beverly, MA, USA), caspase-3, NOX 2, TLR4, iNOS (1:1000, Abcam, Cambridge, UK), cleaved caspase-3 (1:500 for Western blotting, Cell signaling Technology), BMPR1A (Santa Cruz, Dallas, Texas, USA), housekeeping GAPDH (1:10000, Santa Cruz), nitrotyrosine (1:500, Abcam), BMP4 (1:500, Sigma), phosphorylated eNOS at Ser^{1177} (p-eNOS-Ser^{1177}; 1:500, Cell Signaling Technology) and eNOS (1:1000, BD Transduction Laboratory, Oxford, UK). After overnight incubation at 4 °C, the membranes were washed three times in TBS-T and incubated with appropriate secondary antibodies conjugated to horseradish peroxidase for two hours at room temperature. The membranes were developed with enhanced chemiluminescence (ECL) plus Western blotting detection system (Amersham, Buckinghamshire, UK). The densitometric analysis was performed using

Quantity One 1D analysis software (Bio-rad). The protein levels were normalized to the housekeeping protein GAPDH and expressed relative to control.

ROS production

ROS production in the *en face* endothelium of mouse aortae was measured by dihydroethidium (DHE, D1168, Invitrogen, Carlsbad,USA) by confocal microscopy (Choy et al., 2017). In brief, the aortic rings were incubated in normal physiological solution (NPSS, composition in mM: NaCl 140, KCl 5, $CaCl_2$ 1, $MgCl_2$ 1, glucose 10 and HEPES 5) containing 5 μM DHE (Molecular Probes, Eugene, OR, USA) during 15 minutes at 37 ℃ and then washed twice in PBS. The aortae rings were cut open and the preparations were placed upside down between two coverslips on the microscope. Fluorescence intensity was measured with a confocal microscope [Leica TCS SP5 II (Leica Microsystems, Mannheim, Germany)] with 515-nm excitation and 585-nm long pass filters. Background autofluorescence of elastin was measured at excitation 488 nm and emission 520 nm separately to avoid overlapping of the emission spectra. DHE fluorescence intensity was evaluated with Leica LAS-AF software (version 2.6.0.7266) and is represented as fold changes in fluorescence intensity relative to control.

Detection of superoxide anion formation

The amount of superoxide anions formed was quantified using the lucigenin-enhanced chemiluminescence method (Choy et al., 2017). In short, aortic rings isolated from each groups were pre-incubated for 45 min at 37 °C in Krebs-HEPES buffer (in mM: NaCl 99, $NaHCO_3$ 25, KCl 4.7, KH_2PO_4 1, $MgSO_4$ 1.2, glucose 11, $CaCl_2$ 2.5 and Na-HEPES 20) in the presence of diethylthiocarbamic acid (DETCA, 1 mM) to inactivate superoxide dismutase (SOD) and β-nicotinamide adenine dinucleotide phosphate (β-NADPH, 0.1 mM) as a substrate for NADPH oxidase. The inhibitor of NADPH oxidase; diphenylene iodonium (DPI; 5 mM) was used as a

positive control. Then, the rings were transferred to a 96-well Optiplate containing lucigenin (5 mM, Sigma Aldrich) and β-NADPH (0.1 mM, Sigma Aldrich) in 300 ml of Krebs-HEPES buffer per well and the signal was read with Hidex plate CHAMELEONTM V (SisLab, Turku, Finland) in luminescent detection mode for repetitive measurements of photo emission at 30 seconds intervals over 20 minutes. Upon completion of the measurements, the rings were dried during 48 hours at 65 °C and weighed. The data are expressed as average counts per mg of vessel dry weight.

Statistical analysis

Results are shown as means ± SEM; *n* reflects the number of individual experiments. Concentration-response data were fitted to a sigmoidal curve using non-linear regression with a statistical software [GraphPad Prism version 4 (GraphPad Software Inc., San Diego, CA, USA)]. Statistical significance was determined using Student's *t*-test for unpaired observations and, for multiple value comparison, one-way analysis of variance (ANOVA) followed by Bonferroni's multiple comparison test. A value of P less than 0.05 was considered to indicate statistically significant differences.

Chemicals and materials

The chemicals and pharmacological agents used are listed in Table 1, Supplemental data. The concentrations of pharmacological agents used were selected from past experience in the laboratory or from the literature.

Results

LPS-induces apoptosis in HUVECs by engaging the TLR4 and BMP4 signalling pathways independently.

Western blotting was performed to investigate the mechanism underlying LPS-induced cell apoptosis in HUVECs. TLR4 activation by LPS in HUVECs was inhibited significantly by TAK242 but not affected by the other inhibitors tested (Fig. 2A&B). The phosphorylation of p38 protein in response to LPS was prevented by SB202190, noggin, TAK242 and apocynin without changes in total p38 protein presence (Fig. 2A&C). Similarly, the phosphorylation of JNK stimulated by LPS was inhibited by SP600125, noggin, TAK242 and apocynin without changes in total JNK protein presence (Fig. 2A&D). Furthermore, LPS upregulated BMP4 and BMPR1A (Fig. 2A, E & F) protein levels; these effects of LPS were inhibited by noggin but not by SB202190, SP600125, TAK242, aminoguanidine or apocynin. LPS reduced both the total eNOS (Fig. 3A&B) as well as the phosphorylated eNOS (Fig. 3A&C) protein levels with no difference in their ratio, while increasing iNOS levels (Fig. 3A&D) and caspase-3 activation (Fig. 3A&E); these effects of LPS were reversed by all the inhibitors tested. Noggin, TAK242 and apocynin inhibited the upregulation of nicotinamide adenine dinucleotide phosphate oxidase subunit 2 (NOX2) caused by LPS (Fig. 3A&F). Similarly, flowcytometry showed that LPS (0.1, 0.5 and 1 μg/mL) significantly increased the percentage of apoptosis (Supplemental Figure 2 A&B) and augmented the presence of cleaved caspase 3 protein (Supplemental Figure 2C) in a concentration-dependent manner compared with control, with 1 μg/mL LPS being the optimal concentration to induce apoptosis in HUVECs.

To determine the link between TLR4 and BMP4 signalling pathways in LPS-induced apoptosis, BMP4-and TLR4-siRNAs were used in HUVECs to knock-down the expression of BMP4 and TLR4, respectively. At 50 nM, TLR4-siRNAs and BMP4siRNAs reduced TLR4 and BMP4 protein presence, respectively, by approximately 60%, compared with scrambled siRNAs (Supplemental Figure 3). The protein presence of TLR4 (Fig. 4A&B) and cleaved caspase 3 (Fig. 4A&E) was reduced significantly in HUVECs transfected with TLR4-siRNAs compared with scrambled siRNAs, in the absence or presence of LPS. The inductions of BMP4 (Fig. 4A&C) and BMPR1A (Fig. 4A&D) protein levels by LPS were similar in both scrambled siRNA and TLR4-siRNA-transfected cells. The siRNAs against BMP4 reduced the LPS-induced increases in BMP4 (Fig. 5A&C), BMPR1A (Fig. 5A &D), and cleaved caspase 3 (Fig. 5A &E) proteins levels, but did not affect that of TLR4 (Fig. 5A &B).

Paeonol reverses LPS-induced inflammation and apoptosis in HUVECs by inhibiting both BMP4 and TLR4 signalling.

Flow-cytometry revealed that in HUVECs, paeonol (0.01, 0.1, 1 μM) in co-treatment with LPS (1 μg/mL) reduced apoptosis (Supplemental Figure 4) in a concentration-dependent manner, with 1 μM exerting the most significant effect. Therefore, paeonol at 1 μM was used in further experiments. Paeonol significantly reduced the elevation in TLR4, BMP4, BMPR1A and cleaved caspase 3 protein levels triggered by LPS in cells treated with scrambled siRNA (Fig 4&5). Silencing of TLR4 abolished the inhibitory effects of paeonol on LPS-induced activation of TLR4 (Fig. 4A&B) and cleaved caspase 3 (Fig. 4A&E). Similarly, silencing of BMP4 abrogated the paeonol-mediated protection against LPS-induced activation of BMP4 (Fig. 5A&C) and cell death (Fig. 5A &E).

To determine the effect of paeonol on the BMP4 signalling cascade leading to activation of cell apoptosis, BMP4-treated HUVECs were co-incubated with paeonol, noggin, SB202190, SP600125, apocynin and TAK242. Western blotting revealed that BMP4-treatment upregulated phosphorylated p38 MAPK (Fig. 6A&B), phosphorylated JNK (Fig. 6A&C), BMPR1A (Fig. 6A&D), cleaved caspase 3 (Fig. 6A&F), and NOX 2 (Fig. 6A&G) while the phosphorylation of eNOS (Fig. 6A&E) was reduced without affecting the total eNOS level; co-treatment with paeonol normalised the presence of these proteins. In addition, Western blotting showed that phosphorylation of p38 MAPK in response to BMP4 was abolished by noggin, SB202190 and apocynin without changes in total p38 protein presence (Fig. 6A&B). Likewise, phosphorylation of JNK stimulated by BMP4 was also prevented by noggin, SP600125 and apocynin without changes in total JNK (Fig. 6A&C). Activation of BMPR1A by BMP4 was inhibited by noggin but not by the other inhibitors tested (Fig. 6A&D). In addition, the downregulation of phosphorylated eNOS (Fig. 6A&E) and the activation of caspase 3 (Fig. 6A&F) by BMP4 were normalised by all inhibitors except for TAK242. NOX2 activation induced by BMP4 was inhibited only by noggin and apocynin (Fig. 6A&G).

Paeonol reduced apoptosis induced by LPS but not by hydrogen peroxide (H_2O_2, 200 μM), which served as oxidative stress inducer and a positive control. (Fig. 7A&B). Paeonol also reversed the changes induced by LPS (1 μg/mL) on the protein levels of TLR4 (Fig. 7C&D), BMP4 (Fig. 7C&E) and cleaved caspase 3 (Fig. 7C&F). No significant changes were observed between the control and the paeonol (1 μM) only groups (Fig. 7).

Paeonol reverses LPS-induced endothelial dysfunction *ex vivo*

The relaxations evoked by the endothelium-dependent dilator acetylcholine were impaired, compared to the control group, in aortic rings treated with LPS (1 μg/mL) during *ex*

vivo culture in DMEM for 24 hours (Figure 8A-C). Co-treatment with paeonol (0.1, 0.3 and 1 μM) for 24 hours (Supplemental Figure 5A) significantly reversed this impairment in a concentration-dependant manner, with paeonol at 1 μM being a fully effective concentration (Fig. 8A). To elucidate the signalling pathway involved in LPS-induced endothelial dysfunction, the effects of the following pharmacological inhibitors were tested: SB202190 (10 μM), SP600125 (10 μM), TAK242 (1 μM), aminoguanidine (100 μM), noggin (100 ng/mL), and apocynin (20 μM). These inhibitors significantly reversed the impairment of the relaxation to acetylcholine induced by LPS (Fig. 8B-C). By contrast, co-incubation with indomethacin (10 μM, non-selective cyclooxygenase inhibitor) for 24 hours did not reduce the impairment of acetylcholine-induced relaxations induced by LPS (Supplemental Figure 5B&C).

To determine whether or not the endothelium-protective effect of paeonol is BMP4-dependent, BMP4 at 100 ng/mL was used to induce impairment of the relaxation to acetylcholine. The data showed that 24 hours exposure to BMP4 attenuated the response to the muscarinic agonist in mouse aortae and this inhibition was reversed by co-treatment with paeonol, noggin, apocynin, SB202190 and SP600125 (Fig. 8D-F). Relaxations to sodium nitroprusside (exogenous NO-donor) were comparable in the different experimental groups (Supplemental Figure 5D-I).

Paeonol protects against LPS-induced endothelial dysfunction *in vivo*

Aortae of mice exposed to LPS (15 mg/kg/i.p) exhibited attenuated acetylcholine-induced relaxations (Fig. 9A); this impairment was reversed by co-treatment with paeonol (Fig. 9A), noggin (Fig. 9B) or TAK242 (Fig. 9B). Sodium nitroprusside-induced relaxations were unchanged (Supplemental Figure 1C-E). Mice exposed to LPS also showed elevated protein

levels of BMP4 (Fig. 9C), TLR4 (Fig. 9D), iNOS (Fig. 9E), and cleaved caspase 3 (Fig. 9F), and these effects were reversed by paeonol, noggin and TAK242.

Next, ROS levels were determined in mouse aortae. ROS formation and superoxide anion levels in the *en face* endothelium were significantly increased in mice exposed to LPS compared to the control group, as shown by the intensity of DHE fluorescence staining (Fig 9 G&H) and lucigenin-enhanced chemiluminescence (Fig 9I), respectively. Co-treatment with paeonol reduced the LPS-stimulated increase in ROS formation. Similarly, treatment with noggin and TAK242 normalized the elevated ROS production in mice exposed to LPS. The ROS level in the paeonol only group was similar to that observed in aortae of the control group (Fig 9 H&I).

Discussion

The present study was undertaken to investigate the anti-inflammatory properties and mechanism of actions of paeonol in preventing the endothelial dysfunction induced by LPS. The major finding of the present study is that paeonol attenuated LPS induced-endothelial dysfunction and apoptosis by inhibiting the BMP4 pathway, independently of TLR4 signalling.

The endothelium forms a protective single cellular layer between the intravascular and extravascular cells/tissues; it plays an important role in regulating vascular tone in normal and pathological states (Cines et al., 1998). BMP4 is expressed in endothelial cells and can be induced by oscillatory shear stress (Sorescu et al., 2003). BMP4 significantly activate local inflammatory responses and is overexpressed in the myocardial tissue and aortae of obese mice (Wu et al., 2015). The pro-apoptotic effect of BMP4 in endothelial cells is mediated by type I receptors [BMPR1A, also known as activing receptor-like kinase 3 (ALK3)] which triggers smad-independent pathways, leading to activation of NADPH oxidases producing ROS and p38 MAPK/JNK (Tian et al., 2012). The present results show that BMP4 is involved in the apoptosis and endothelial dysfunction induced by LPS in human endothelial cells and the mouse aorta. This conclusion is based on the following observations: (a) LPS increased the protein presence of both BMP4 and BMPR1A and this was inhibited by noggin; (b) inhibition of BMP4 reduced LPS-induced inflammation, apoptosis and endothelial dysfunction. The present findings also demonstrate that silencing of BMP4 inhibits LPS-induced apoptosis without affecting the LPS-induced augmentation of TLR4. By contrast, silencing of TLR4 does not affect the LPS-induced upregulation of BMP4, suggesting that BMP4 activation by LPS is independent of TLR4 signalling.

In the present study, LPS-induced apoptosis in the HUVECs was reversed concentration-dependently by paeonol. Similarly, paeonol reduced the apoptotic activity in cardiac myocytes following myocardial infarction (Li et al., 2016) and suppressed endothelial cell apoptosis induced by oxidized low-density lipoprotein *via* activation of the LOX-1/p38MAPK/NF-κβ pathway (Bao et al., 2013). However, H_2O_2-induced cell apoptosis was not reversed by paeonol, suggesting that the anti-apoptotic effect of paeonol does not involve its anti-oxidant actions (Bao et al., 2013). Mediators of MAPK signalling induced by LPS play an important role in cellular dysfunction, whereby p38 and JNK are activated in response to stresses such as apoptosis, and ERK is involved in growth responses (Frey and Finlay, 1998; Kacimi et al., 2011). In endothelial cells, p38 MAPK and JNK/SAPK induce inflammation and cell apoptosis by modulating ROS-production (Griendling et al., 2000; Junttila et al., 2008). The present Western blot analysis shows that paeonol reduces the presence of BMP4 protein as well as several downstream kinases and transcription factors (JNK, p38 MAPK, iNOS, NOX2) activated by LPS or BMP4, and eventually attenuates the increase in cleaved caspase 3. Paeonol also reduced the NOX2 protein level and superoxide anion production stimulated by LPS and BMP4, suggesting that the anti-oxidant effect of paeonol is a consequences of its inhibitory effect on TLR4 and BMP4. Silencing of TLR4 and BMP4 prevented the protective effects of paeonol on LPS-induced upregulation cleaved caspase 3 independently, indicating that the anti-apoptotic effect of paeonol is partially mediated by TLR4 and BMP4 signalling. In addition, silencing of TLR4 did not prevent the inhibitory effect of paeonol on the activation of BMP4 signalling by LPS, demonstrating that the compound modulates these two pathways independently The present experiments do not allow to define the actual molecular targets of paeonol to curtail LPS-induced inflammation by independently inhibiting both TLR4 and BMP4. However, since the downstream signalling of BMP4 and TLR4 is similar, expectedly, both BMP4 and TLR4 activation induced ROS, MAPK and cleaved caspase 3.

Endothelial dysfunction is one of the common features of sepsis and other inflammatory cardiovascular diseases (Didion et al., 2004). In addition, TLR4 activation by LPS increases the expression of adhesion molecules which recruits leucocytes (Lee et al., 2012) and promotes the transcription of NADPH oxidase, resulting in elevated reactive oxidative stress and uncoupling of eNOS leading to endothelial dysfunction in arteries (Liang et al., 2013). Paeonol alleviates oxidative stress, inflammation, and fibrosis in the lungs induced by bleomycin *in vivo* and suppresses TGF-β1-induced fibrotic responses *in vitro* by inhibiting MAPKs/Smad3 signalling (Liu et al., 2017). The improvement in endothelial function following treatment with paeonol *in vivo* was accompanied by normalization of iNOS and cleaved caspase 3 protein levels as well as of ROS production, increased by LPS. These findings are in line with the earlier finding that iNOS-generated NO suppressed eNOS expression and activity of guanylate cyclase activity, thereby causing a state of endothelial dysfunction (Chauhan et al., 2003). However, this dysfunction is not likely due to tolerance of the vascular smooth muscle cells to iNOS-produced NO, since LPS treatment has a minor effect on responses to an NO donor (Chauhan et al., 2003), an interpretation in line with the current experiments with sodium nitroprusside. By inhibiting LPS-induced exaggerated NO production by iNOS, paeonol may additionally restore eNOS activity and improve endothelial dysfunction.

Although the *ex vivo* and *in vivo* validation of *in vitro* findings were performed in systems from two different species, with the former two being carried out on C57BL/6J mouse aortae and the latter on human HUVECs, the results obtained from the *ex vivo* and *in vivo* experiments were in accordance with the findings obtained on human endothelial cells *in vitro*. Hence, the present findings demonstrate, across different species and with relevance to humans, the inhibitory effects of paeonol against LPS-induced apoptosis and endothelial dysfunction are due in part to BMP4 activation independently of TLR4 stimulation. The results suggest that

pharmacological modulation of BMP4 activation by paeonol may provide a novel strategy for treating inflammation-related diseases such as diabetes mellitus and obesity, in particular those affecting endothelial function.

Authorship Contributions:

Participated in research design: Choy, Lau, Murugan, Vanhoutte, Mustafa

Conducted experiments*:* Choy

Contributed new reagents or analytic tools: Mustafa

Performed data analysis*:* Choy

Wrote or contributed to the writing of the manuscript: Choy, Lau, Murugan, Vanhoutte, Mustafa

References

Bannerman DD and Goldblum SE (1999) Direct effects of endotoxin on the endothelium: barrier function and injury. *Laboratory investigation; a journal of technical methods and pathology* **79**:1181-1199.

Bannerman DD and Goldblum SE (2003) Mechanisms of bacterial lipopolysaccharide-induced endothelial apoptosis. *Am J Physiol Lung Cell Mol Physiol* **284**:L899-914.

Bao MH, Zhang YW and Zhou HH (2013) Paeonol suppresses oxidized low-density lipoprotein induced endothelial cell apoptosis via activation of LOX-1/p38MAPK/NF-kappaB pathway. *Journal of ethnopharmacology* **146**:543-551.

Chauhan SD, Seggara G, Vo PA, Macallister RJ, Hobbs AJ and Ahluwalia A (2003) Protection against lipopolysaccharide-induced endothelial dysfunction in resistance and conduit vasculature of iNOS knockout mice. *FASEB J* **17**:773-775.

Chen D, Zhao M and Mundy GR (2004) Bone morphogenetic proteins. *Growth Factors* **22**:233-241.

Choy KW, Lau YS, Murugan D and Mustafa MR (2017) Chronic treatment with paeonol improves endothelial function in mice through inhibition of endoplasmic reticulum stress-mediated oxidative stress. *PLoS One* **12**:1-18.

Choy KW, Mustafa MR, Lau YS, Liu J, Murugan D, Lau CW, Wang L, Zhao L and Huang Y (2016) Paeonol protects against endoplasmic reticulum stress-induced endothelial dysfunction via AMPK/PPARdelta signaling pathway. *Biochem Pharmacol* **116**:51-62.

Cines DB, Pollak ES, Buck CA, Loscalzo J, Zimmerman GA, McEver RP, Pober JS, Wick TM, Konkle BA, Schwartz BS, Barnathan ES, McCrae KR, Hug BA, Schmidt AM and Stern DM (1998) Endothelial cells in physiology and in the pathophysiology of vascular disorders. *Blood* **91**:3527-3561.

Csiszar A, Ahmad M, Smith KE, Labinskyy N, Gao Q, Kaley G, Edwards JG, Wolin MS and Ungvari Z (2006) Bone morphogenetic protein-2 induces proinflammatory endothelial phenotype. *The American journal of pathology* **168**:629-638.

Csiszar A, Labinskyy N, Smith KE, Rivera A, Bakker EN, Jo H, Gardner J, Orosz Z and Ungvari Z (2007) Downregulation of bone morphogenetic protein 4 expression in coronary arterial endothelial cells: role of shear stress and the cAMP/protein kinase A pathway. *Arterioscler Thromb Vasc Biol* **27**:776-782.

Cuschleri J, Gourlay D, Garcia I, Jelacic S and Maier RV (2003) Endotoxin-induced endothelial cell proinflammatory phenotypic differentiation requires stress fiber polymerization. *Shock* **19**:433-439.

Didion SP, Kinzenbaw DA, Fegan PE, Didion LA and Faraci FM (2004) Overexpression of CuZn-SOD prevents lipopolysaccharide-induced endothelial dysfunction. *Stroke; a journal of cerebral circulation* **35**:1963-1967.

Everhardt Queen A, Moerdyk-Schauwecker M, McKee LM, Leamy LJ and Huet YM (2016) Differential Expression of Inflammatory Cytokines and Stress Genes in Male and Female Mice in Response to a Lipopolysaccharide Challenge. *PLoS One* **11**:e0152289.

Fan HY, Qi D, Yu C, Zhao F, Liu T, Zhang ZK, Yang MY, Zhang LM, Chen DQ and Du Y (2016) Paeonol protects endotoxin-induced acute kidney injury: potential mechanism of inhibiting TLR4-NF-kappaB signal pathway. *Oncotarget* **7**:39497-39510.

Frey EA and Finlay BB (1998) Lipopolysaccharide induces apoptosis in a bovine endothelial cell line via a soluble CD14 dependent pathway. *Microb Pathog* **24**:101-109.

Griendling KK, Sorescu D, Lassegue B and Ushio-Fukai M (2000) Modulation of protein kinase activity and gene expression by reactive oxygen species and their role in vascular physiology and pathophysiology. *Arterioscler Thromb Vasc Biol* **20**:2175-2183.

Hsieh CL, Cheng CY, Tsai TH, Lin IH, Liu CH, Chiang SY, Lin JG, Lao CJ and Tang NY (2006) Paeonol reduced cerebral infarction involving the superoxide anion and microglia activation in ischemia-reperfusion injured rats. *Journal of ethnopharmacology* **106**:208-215.

Hu J, Li YL, Li ZL, Li H, Zhou XX, Qiu PC, Yang Q and Wang SW (2012) Chronic supplementation of paeonol combined with danshensu for the improvement of vascular reactivity in the cerebral basilar artery of diabetic rats. *International journal of molecular sciences* **13**:14565-14578.

Junttila MR, Li SP and Westermarck J (2008) Phosphatase-mediated crosstalk between MAPK signaling pathways in the regulation of cell survival. *FASEB J* **22**:954-965.

Kacimi R, Giffard RG and Yenari MA (2011) Endotoxin-activated microglia injure brain derived endothelial cells via NF-kappaB, JAK-STAT and JNK stress kinase pathways. *J Inflamm (Lond)* **8**:7.

Lau CH, Chan CM, Chan YW, Lau KM, Lau TW, Lam FC, Law WT, Che CT, Leung PC, Fung KP, Ho YY and Lau CB (2007) Pharmacological investigations of the anti-diabetic effect of Cortex Moutan and its active component paeonol. *Phytomedicine : international journal of phytotherapy and phytopharmacology* **14**:778-784.

Lee H, Lee G, Kim H and Bae H (2013) Paeonol, a major compound of moutan cortex, attenuates Cisplatin-induced nephrotoxicity in mice. *Evidence-based complementary and alternative medicine : eCAM* **2013**:310989.

Lee IT, Shih RH, Lin CC, Chen JT and Yang CM (2012) Role of TLR4/NADPH oxidase/ROS-activated p38 MAPK in VCAM-1 expression induced by lipopolysaccharide in human renal mesangial cells. *Cell Commun Signal* **10**:33.

Li H, Dai M and Jia W (2009) Paeonol attenuates high-fat-diet-induced atherosclerosis in rabbits by anti-inflammatory activity. *Planta medica* **75**:7-11.

Li H, Song F, Duan LR, Sheng JJ, Xie YH, Yang Q, Chen Y, Dong QQ, Zhang BL and Wang SW (2016) Paeonol and danshensu combination attenuates apoptosis in myocardial infarcted rats by inhibiting oxidative stress: Roles of Nrf2/HO-1 and PI3K/Akt pathway. *Scientific reports* **6**:23693.

Li H, Xie YH, Yang Q, Wang SW, Zhang BL, Wang JB, Cao W, Bi LL, Sun JY, Miao S, Hu J, Zhou XX and Qiu PC (2012) Cardioprotective effect of paeonol and danshensu combination on isoproterenol-induced myocardial injury in rats. *PLoS One* **7**:e48872.

Li YJ, Bao JX, Xu JW, Murad F and Bian K (2010) Vascular dilation by paeonol-a mechanism study. *Vascular pharmacology* **53**:169-176.

Li Z, Wang J, Wang Y, Jiang H, Xu X, Zhang C, Li D, Xu C, Zhang K, Qi Y, Gong X, Tang C, Zhong N and Lu W (2014) Bone morphogenetic protein 4 inhibits liposaccharide-induced inflammation in the airway. *European journal of immunology* **44**:3283-3294.

Liang CF, Liu JT, Wang Y, Xu A and Vanhoutte PM (2013) Toll-like receptor 4 mutation protects obese mice against endothelial dysfunction by decreasing NADPH oxidase isoforms 1 and 4. *Arterioscler Thromb Vasc Biol* **33**:777-784.

Liu MH, Lin AH, Ko HK, Perng DW, Lee TS and Kou YR (2017) Prevention of Bleomycin-Induced Pulmonary Inflammation and Fibrosis in Mice by Paeonol. *Front Physiol* **8**:193.

Lockyer P, Mao H, Fan Q, Li L, Yu-Lee LY, Eissa NT, Patterson C, Xie L and Pi X (2017) LRP1-Dependent BMPER Signaling Regulates Lipopolysaccharide-Induced Vascular Inflammation. *Arterioscler Thromb Vasc Biol* **37**:1524-1535.

Mann DL, Topkara VK, Evans S and Barger PM (2010) Innate immunity in the adult mammalian heart: for whom the cell tolls. *Transactions of the American Clinical and Climatological Association* **121**:34-50; discussion 50-31.

Meng-Han Liu H-FL, Tzong-Shyuan Lee, Yu Ru Kou (2014) Therapeutic effects and mechanisms of paeonol on cigarette smoke-induced lung inflammation *The FASEB Journal* **28**.

Miriyala S, Gongora Nieto MC, Mingone C, Smith D, Dikalov S, Harrison DG and Jo H (2006) Bone morphogenic protein-4 induces hypertension in mice: role of noggin, vascular NADPH oxidases, and impaired vasorelaxation. *Circulation* **113**:2818-2825.

Shi X, Chen YH, Liu H and Qu HD (2016) Therapeutic effects of paeonol on methyl-4-phenyl-1,2,3,6-tetrahydropyridine/probenecid-induced Parkinson's disease in mice. *Mol Med Rep* **14**:2397-2404.

Sorescu GP, Sykes M, Weiss D, Platt MO, Saha A, Hwang J, Boyd N, Boo YC, Vega JD, Taylor WR and Jo H (2003) Bone morphogenic protein 4 produced in endothelial cells by oscillatory shear stress stimulates an inflammatory response. *The Journal of biological chemistry* **278**:31128-31135.

Sun GP, Wang H, Xu SP, Shen YX, Wu Q, Chen ZD and Wei W (2008) Anti-tumor effects of paeonol in a HepA-hepatoma bearing mouse model via induction of tumor cell apoptosis and stimulation of IL-2 and TNF-alpha production. *European journal of pharmacology* **584**:246-252.

Tian XY, Yung LH, Wong WT, Liu J, Leung FP, Liu L, Chen Y, Kong SK, Kwan KM, Ng SM, Lai PB, Yung LM, Yao X and Huang Y (2012) Bone morphogenic protein-4 induces endothelial cell apoptosis through oxidative stress-dependent p38MAPK and JNK pathway. *Journal of molecular and cellular cardiology* **52**:237-244.

Tseng YT, Hsu YY, Shih YT and Lo YC (2012) Paeonol attenuates microglia-mediated inflammation and oxidative stress-induced neurotoxicity in rat primary microglia and cortical neurons. *Shock* **37**:312-318.

Wu T, Ling Q-Y, Zhong C, Wang T-X, Wang L-L, Wang X-Y, Su Z-L and Zong G-J (2015) Expression of BMP4 in myocardium and vascular tissue of obese mice. *Journal of Inflammation* **12**:8.

Footnotes

This work was supported by Fundamental Research Grant Scheme (FRGS): Project code FP021-2016 (Reference code: FRGS/1/2016/SKK10/UM/01/1).

Figure legends

Fig. 1: Chemical structure of paeonol.

Fig. 2: (A) Western blots and (B-F) quantitative data showing protein presences in human umbilical vein endothelial cells (HUVECs) treated with lipopolysaccharides (LPS, 1 μg/mL) and paeonol (1μM). Results are means ± SEM of four separate experiments. *P<0.05 compared with control, # P<0.05 compared with LPS.

Fig. 3: (A) Western blots and (B-F) quantitative data showing protein presences in human umbilical vein endothelial cells (HUVECs) treated with lipopolysaccharides (LPS, 1 μg/mL) and paeonol (1μM). Results are means ± SEM of four separate experiments. *P<0.05 compared with control, # P<0.05 compared with LPS.

Fig. 4: Effects of toll-like receptor 4 (TLR4) knock-down on the paeonol- induced suppression of pro-inflammatory and apoptotic markers induced by lipopolysaccharides (LPS). TLR4 siRNA (50 nM/well) were transfected into human umbilical vein endothelial cells (HUVECs) for 48 hours. Transfected cells were then exposed to LPS (1 μg/mL) and paeonol (1 μM) for 24 hours. Results are means ± SEM of four separate experiments; *P<0.05 vs. control siRNA, # P<0.05 vs. siRNA control + LPS, Δ P<0.05 vs. siRNA TLR4, ϕ P<0.05 vs. siRNA TLR4 + LPS.

Fig. 5: Effects of bone morphogenic protein-4 (BMP4) knock-down on the paeonol- induced suppression of pro-inflammatory and apoptotic markers induced by lipopolysaccharides (LPS). BMP4 siRNA (50 nM/well) were transfected into human umbilical vein endothelial cells (HUVECs) for 72 hours, respectively. Transfected cells were then exposed to LPS (1 μg/mL)

and paeonol (1 μM) for 24 hours. Results are means ± SEM of four separate experiments; *P<0.05 vs. control siRNA, # P<0.05 vs. siRNA control + LPS, Δ P<0.05 vs. siRNA BMP4, ϕ P<0.05 vs. siRNA BMP4 + LPS.

Fig. 6: (A) Western blots and (B-G) quantitative data showing protein presences in human umbilical vein endothelial cells (HUVECs) treated with bone morphogenic protein-4 (BMP4, 100 ng/mL) and paeonol (1μM). Results are means ± SEM of four separate experiments. *P<0.05 compared with control, # P<0.05 compared with BMP4.

Fig. 7: In HUVECs, paeonol reduced apoptosis induced by 24 hours-exposure to lipopolysaccharides (LPS, 1 μg/mL) but not hydrogen peroxide (H_2O_2, 200 μM). (A) Flow cytometry dot plots showing percentage of apoptotic cells in human umbilical vein endothelial cells (HUVECs) treated with LPS (1 μg/ml) or H_2O_2 (200 μM) and paeonol (1 μM). In each dot plot, the upper left quadrant corresponds to necrotic cells; the upper right quadrant contains the late apoptotic cells, positive for Annexin V and propidium iodide (PI); the lower left quadrant shows viable cells, which exclude PI and Annexin V; and the lower right quadrant represents the early apoptotic cells, Annexin V positive and PI negative. (B) Percentage of apoptotic cells quantified by flow cytometry. (C-F) Western blots and quantitative data showing the protein levels of (C&D) toll-like receptor 4 (TLR4), (C&E) bone morphogenic protein-4 (BMP4) and (C&F) cleaved caspase 3 in HUVECs treated with LPS (1 μg/mL) and paeonol (1 μM). Values are means ± SEM from four independent experiments. * P< 0.05 vs. control, #P<0.05 vs. LPS.

Fig. 8: (A) Paeonol (1 μM) improved relaxations to acetylcholine in mouse thoracic aortae incubated with lipopolysaccharides (LPS, 1 μg/mL) in Dulbecco's Modified Eagle's Medium (DMEM) for 24 hours. Co-incubation of LPS with (B) SB202190 (10 μM, p38 inhibitor), SP600125 (10 μM, p-JNK inhibitor,) and TAK242 (1 μM, TLR4 antagonist) or (C)

aminoguanidine 100μM, selective inhibitor of inducible nitric oxide synthase), noggin [100 ng/ml, bone morphogenic protein-4 (BMP4) inhibitor] and apocynin [20 μM, nicotinamide adenine dinucleotide phosphate (NADPH) oxidase inhibitor], for 24 hours improved the impairment of relaxations to acetylcholine induced by 1 μg/mL LPS in mouse aortae. (D) Paeonol (1 μM) improved the impaired response to acetylcholine in aortae exposed to BMP4 (100 ng/mL, in DMEM) for 24 hours. (E) Co-incubation of BMP4 with noggin (BMP4 inhibitor, 100 ng/ml) and apocynin (NADPH oxidase inhibitor, 20 μM) and (F) SB202190 (p38 inhibitor, 10 μM), SP600125 (p-JNK inhibitor, 10 μM) during 24 hours improved acetylcholine-induced relaxation. Results are means± SEM of seven experiments. * $P < 0.05$, compared to control; # $P < 0.05$, compared to LPS and Δ, $P<0.05$ compared to BMP4.

Fig. 9: (A) Paeonol (20 mg/kg/day/oral administration) improved relaxations to acetylcholine in aortae isolated from mice exposed to lipopolysaccharides (LPS, 15 mg/kg/i.p) during 24 hours. (B) Likewise, treatment with noggin (0.5 mg/kg/i.p) and TAK242 (3 mg/kg/ip) improved the response to the muscarinic agonist in mice treated with LPS. Western blots and quantitative data showing (C) bone morphogenic protein-4 (BMP4), (D) toll like receptor 4 (TLR4), (E) inducible nitric oxide synthase (iNOS) protein and (F) cleaved caspase 3 in all groups of mice. (G&H) Representative images and summarized results of superoxide anion production measured in *en face* aortic endothelium and (I) lucigenin-enhanced chemiluminescence in the aortae mice treated with LPS, noggin) and TAK242 for 24 hours. Red: DHE fluorescence (excitation: 515 nm) in the nucleus. Green: autofluorescence of elastin underneath the endothelium (excitation: 488 nm). Lower panel, merged. Bar: 100 μm. The nicotinamide adenine dinucleotide phosphate (NADPH) oxidase inhibitor, diphenyleneiodonium (DPI, 10 mM) abolished the generation of superoxide anions. Results are means± SEM of seven experiments. *$P<0.05$ compared with control, #$P<0.05$ when compared with LPS.

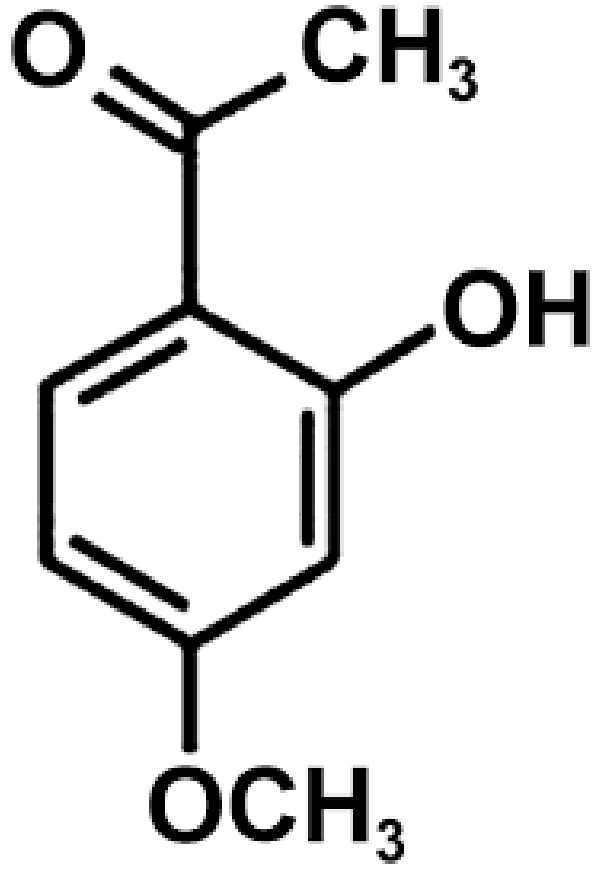

Fig. 1

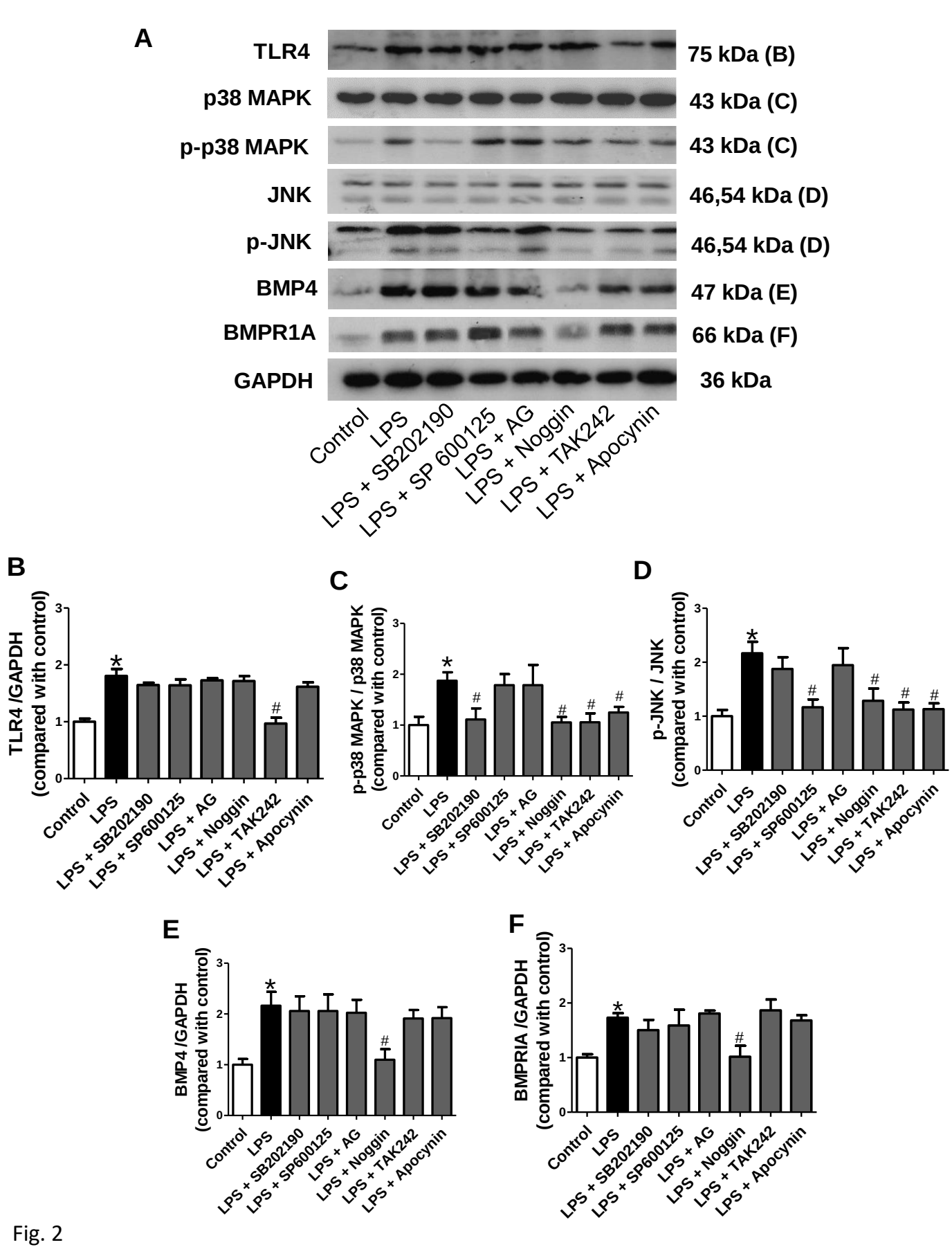
A
TLR4
p38 MAPK
p-p38 MAPK
JNK
p-JNK
BMP4
BMPR1A
GAPDH
75 kDa (B)
43 kDa (C)
43 kDa (C)
46,54 kDa (D)
46,54 kDa (D)
47 kDa (E)
66 kDa (F)
36 kDa
Control
LPS
LPS + SB202190
LPS + SP 600125
LPS + AG
LPS + Noggin
LPS + TAK242
LPS + Apocynin
B
TLR4 /GAPDH (compared with control)
C
p-p38 MAPK / p38 MAPK (compared with control)
D
p-JNK / JNK (compared with control)
E
BMP4 /GAPDH (compared with control)
F
BMPRIA /GAPDH (compared with control)

Fig. 2

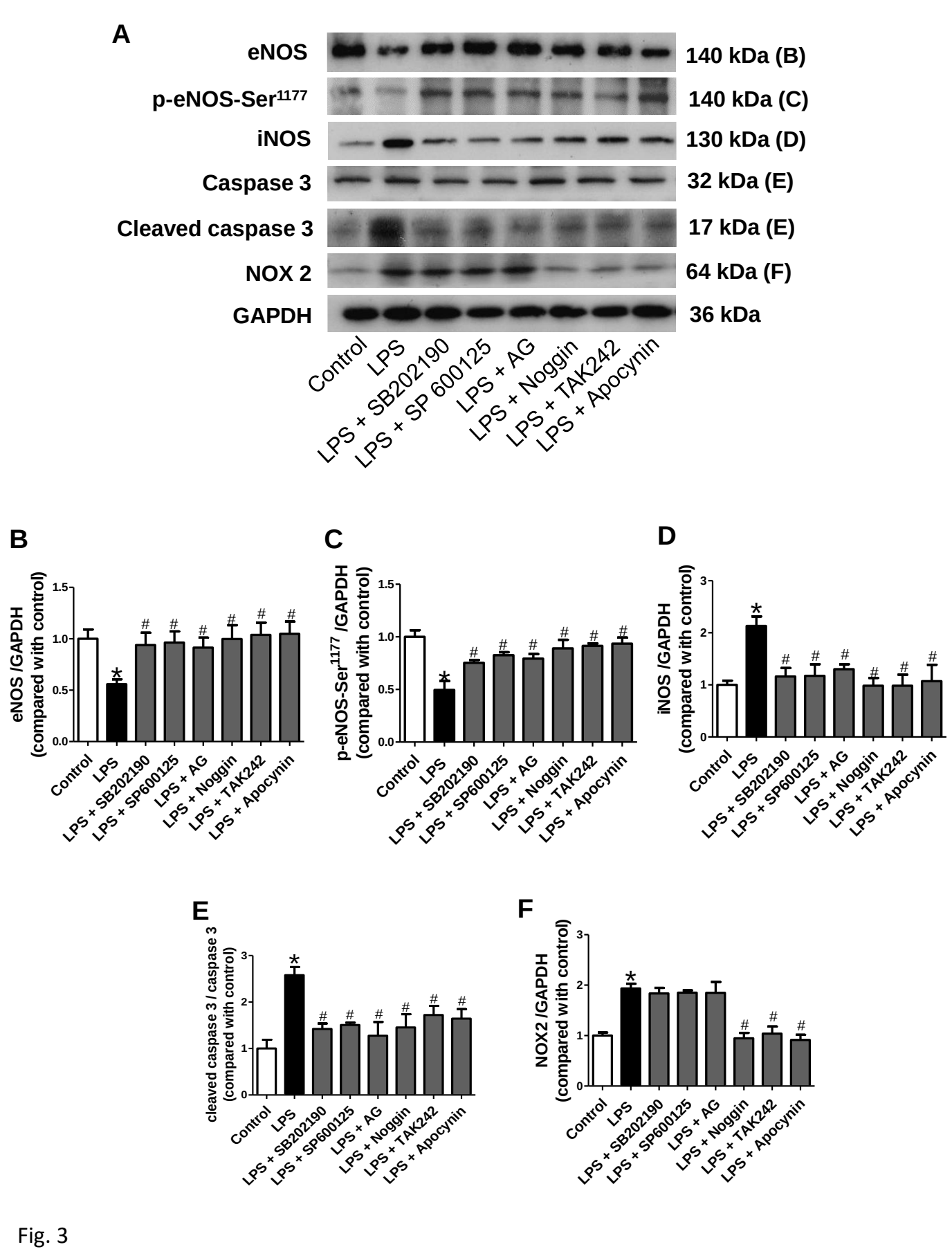
A
eNOS
p-eNOS-Ser1177
iNOS
Caspase 3
Cleaved caspase 3
NOX 2
GAPDH
140 kDa (B)
140 kDa (C)
130 kDa (D)
32 kDa (E)
17 kDa (E)
64 kDa (F)
36 kDa
Control
LPS
LPS + SB202190
LPS + SP 600125
LPS + AG
LPS + Noggin
LPS + TAK242
LPS + Apocynin
B
eNOS /GAPDH (compared with control)
C
p-eNOS-Ser1177 /GAPDH (compared with control)
D
iNOS /GAPDH (compared with control)
E
cleaved caspase 3 / caspase 3 (compared with control)
F
NOX2 /GAPDH (compared with control)

Fig. 3

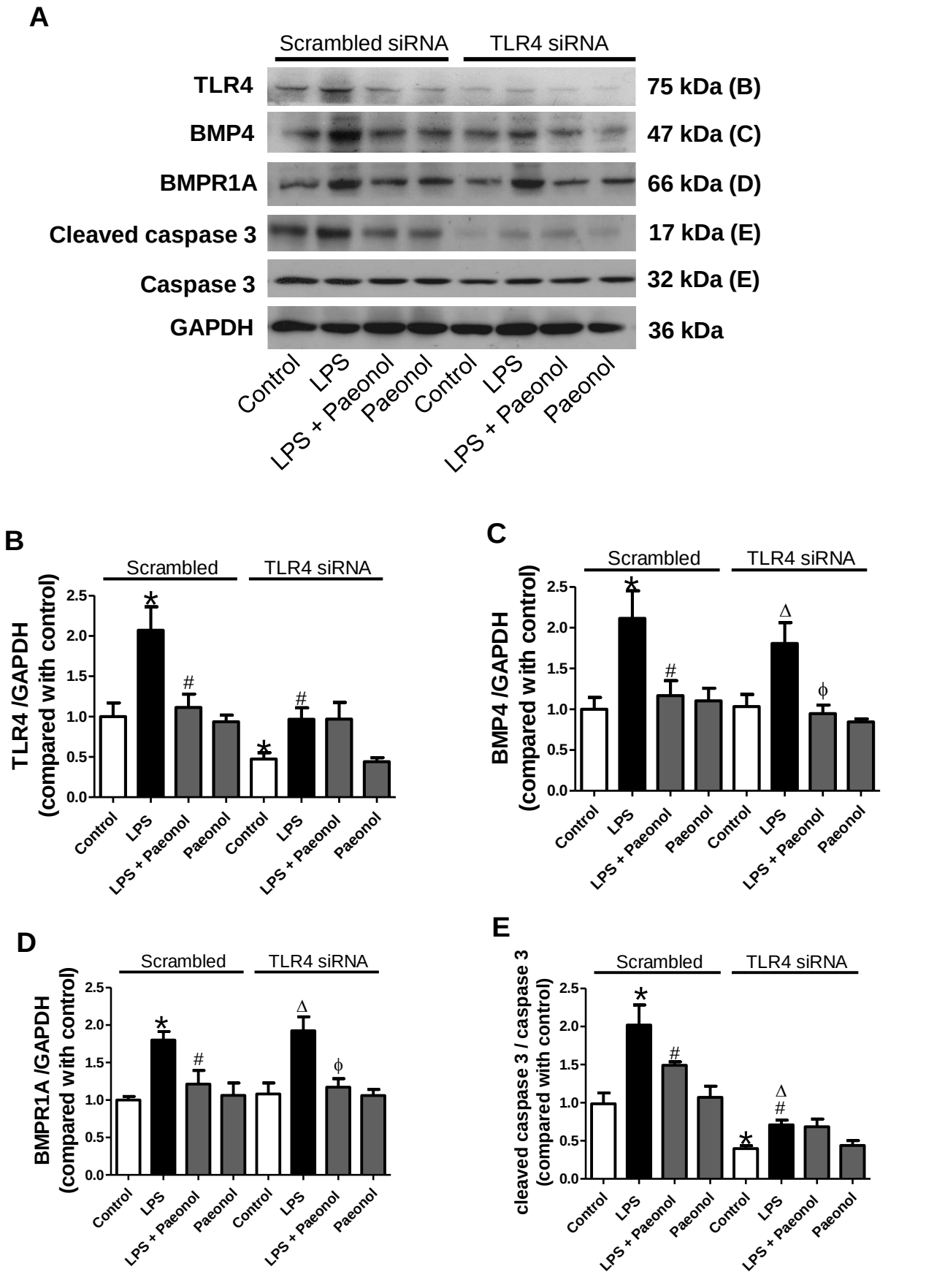
A
Scrambled siRNA
TLR4 siRNA
TLR4
BMP4
BMPR1A
Cleaved caspase 3
Caspase 3
GAPDH
75 kDa (B)
47 kDa (C)
66 kDa (D)
17 kDa (E)
32 kDa (E)
36 kDa
Control
LPS
LPS + Paeonol
Paeonol
B
TLR4 /GAPDH (compared with control)
C
BMP4 /GAPDH (compared with control)
D
BMPR1A /GAPDH (compared with control)
E
cleaved caspase 3 / caspase 3 (compared with control)
Scrambled
TLR4 siRNA

Fig. 4

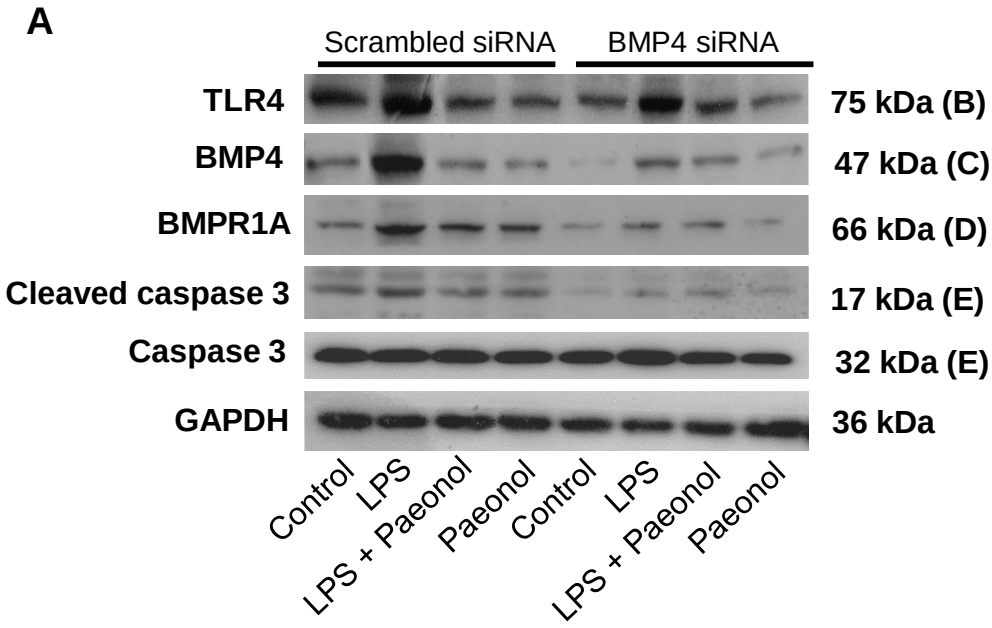
A
Scrambled siRNA
BMP4 siRNA
TLR4
BMP4
BMPR1A
Cleaved caspase 3
Caspase 3
GAPDH
75 kDa (B)
47 kDa (C)
66 kDa (D)
17 kDa (E)
32 kDa (E)
36 kDa
Control
LPS
LPS + Paeonol
Paeonol

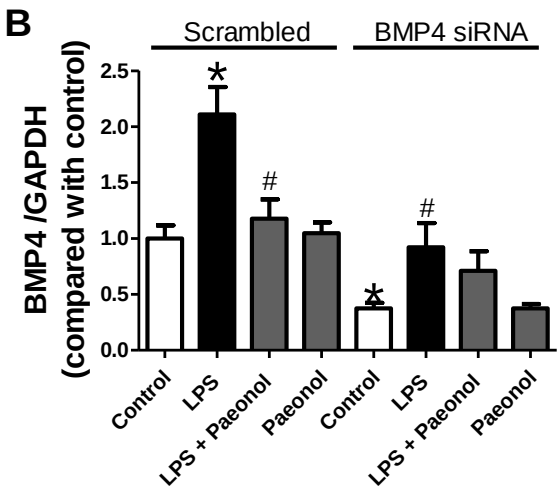
B
Scrambled
BMP4 siRNA
BMP4 /GAPDH
(compared with control)
Control
LPS
LPS + Paeonol
Paeonol

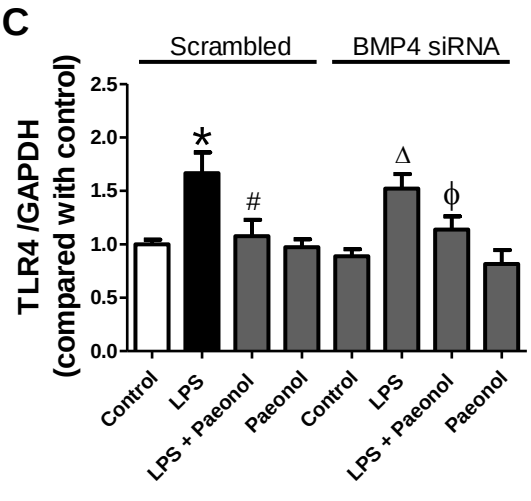
C
Scrambled
BMP4 siRNA
TLR4 /GAPDH
(compared with control)
Control
LPS
LPS + Paeonol
Paeonol

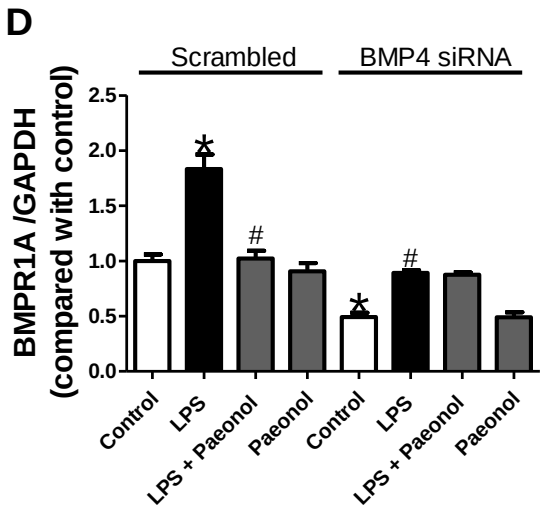
D
Scrambled
BMP4 siRNA
BMPR1A /GAPDH
(compared with control)
Control
LPS
LPS + Paeonol
Paeonol

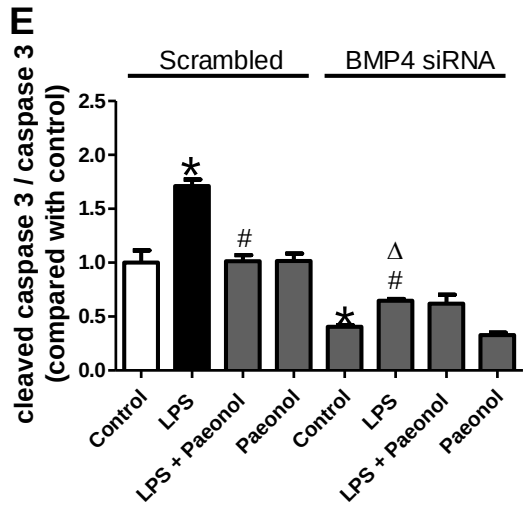
E
Scrambled
BMP4 siRNA
cleaved caspase 3 / caspase 3
(compared with control)
Control
LPS
LPS + Paeonol
Paeonol

Fig. 5

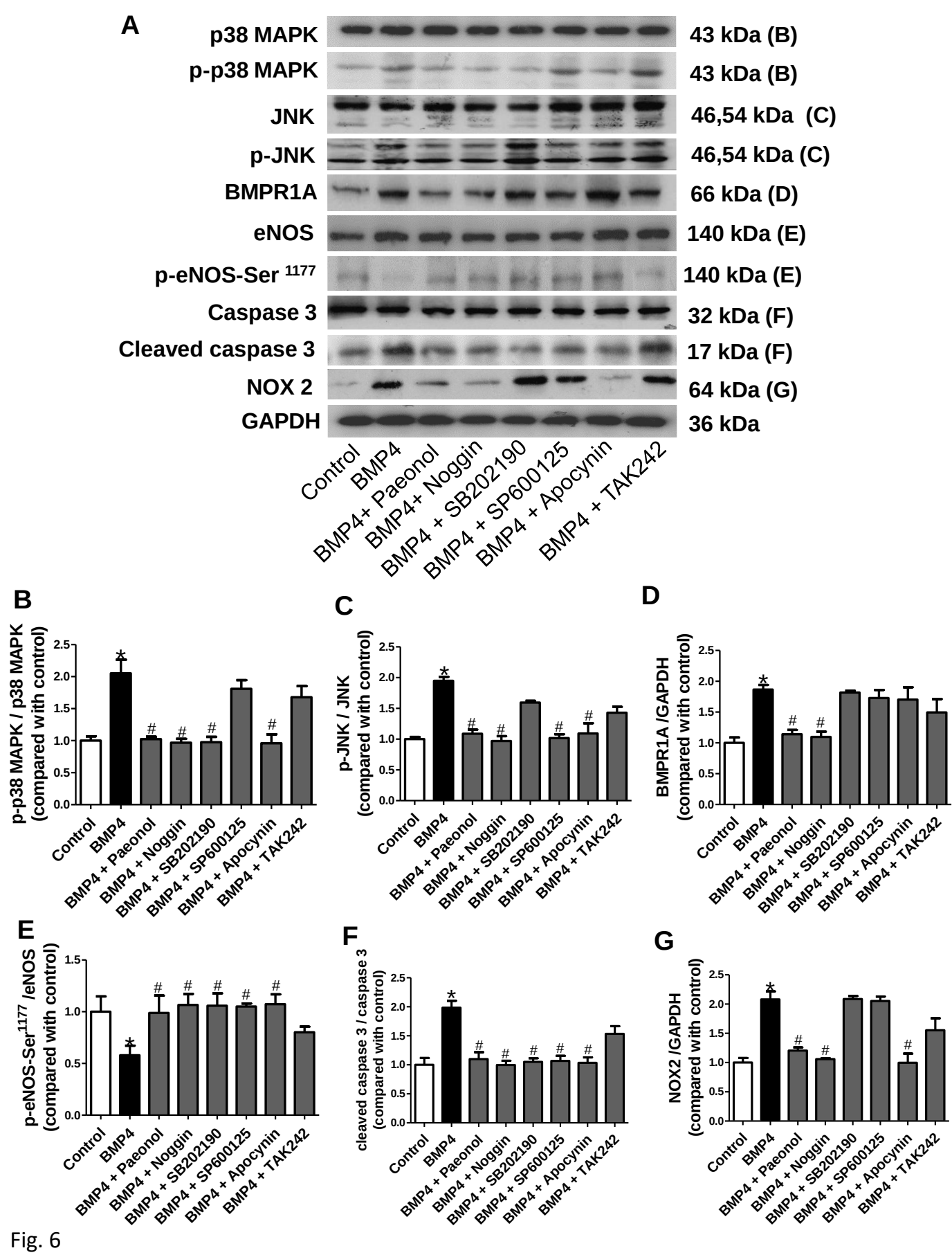
A
p38 MAPK
p-p38 MAPK
JNK
p-JNK
BMPR1A
eNOS
p-eNOS-Ser 1177
Caspase 3
Cleaved caspase 3
NOX 2
GAPDH
43 kDa (B)
43 kDa (B)
46,54 kDa (C)
46,54 kDa (C)
66 kDa (D)
140 kDa (E)
140 kDa (E)
32 kDa (F)
17 kDa (F)
64 kDa (G)
36 kDa
Control
BMP4
BMP4+ Paeonol
BMP4+ Noggin
BMP4 + SB202190
BMP4 + SP600125
BMP4 + Apocynin
BMP4 + TAK242
B
p-p38 MAPK / p38 MAPK (compared with control)
C
p-JNK / JNK (compared with control)
D
BMPR1A /GAPDH (compared with control)
E
p-eNOS-Ser1177 /eNOS (compared with control)
F
cleaved caspase 3 / caspase 3 (compared with control)
G
NOX2 /GAPDH (compared with control)

Fig. 6

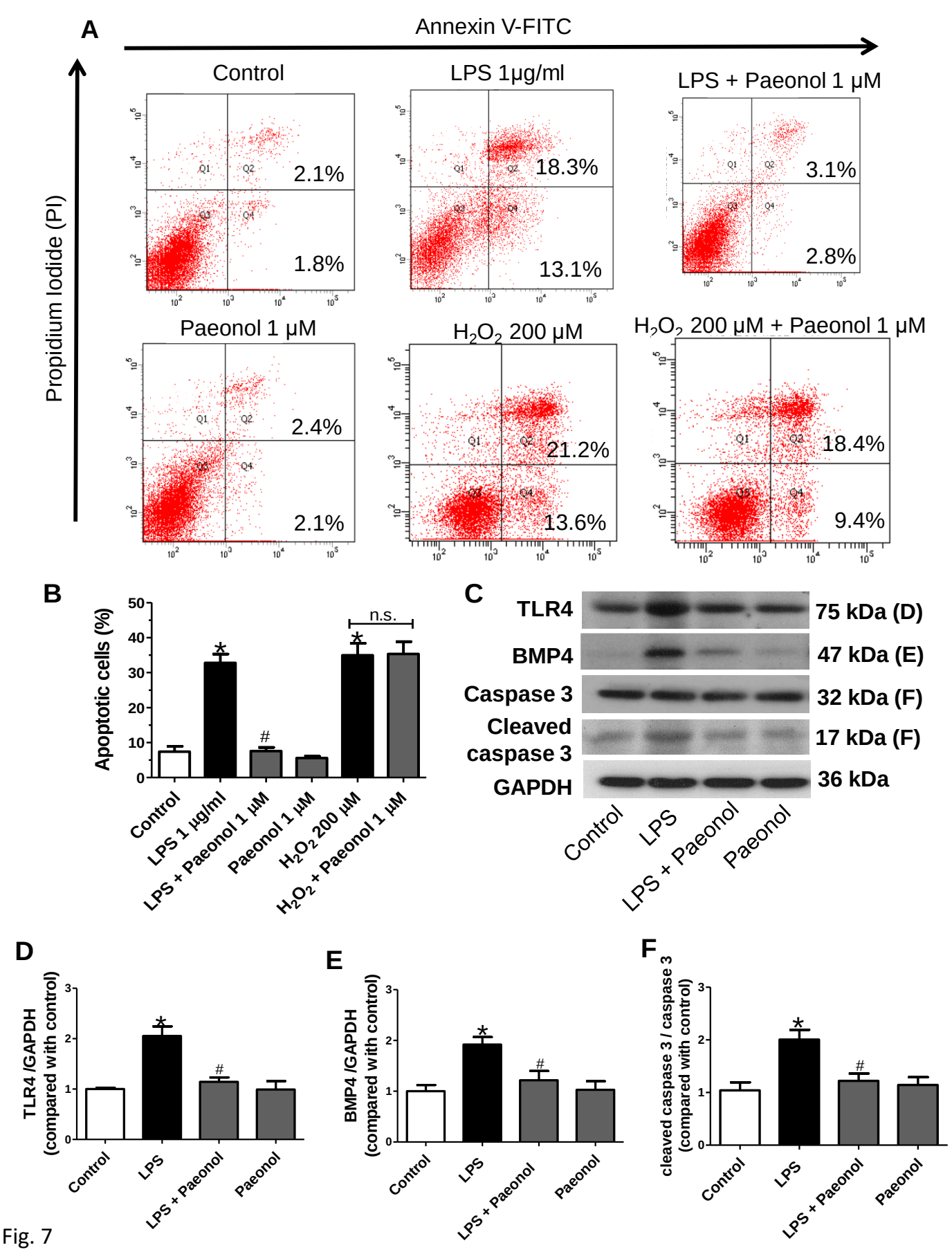
A
Annexin V-FITC
Propidium Iodide (PI)
Control
2.1%
1.8%
LPS 1μg/ml
18.3%
13.1%
LPS + Paeonol 1 μM
3.1%
2.8%
Paeonol 1 μM
2.4%
2.1%
H2O2 200 μM
21.2%
13.6%
H2O2 200 μM + Paeonol 1 μM
18.4%
9.4%
B
Apoptotic cells (%)
n.s.
Control
LPS 1 μg/ml
LPS + Paeonol 1 μM
Paeonol 1 μM
H2O2 200 μM
H2O2 + Paeonol 1 μM
C
TLR4
BMP4
Caspase 3
Cleaved caspase 3
GAPDH
75 kDa (D)
47 kDa (E)
32 kDa (F)
17 kDa (F)
36 kDa
Control
LPS
LPS + Paeonol
Paeonol
D
TLR4 /GAPDH (compared with control)
E
BMP4 /GAPDH (compared with control)
F
cleaved caspase 3 / caspase 3 (compared with control)

Fig. 7

Ex vivo

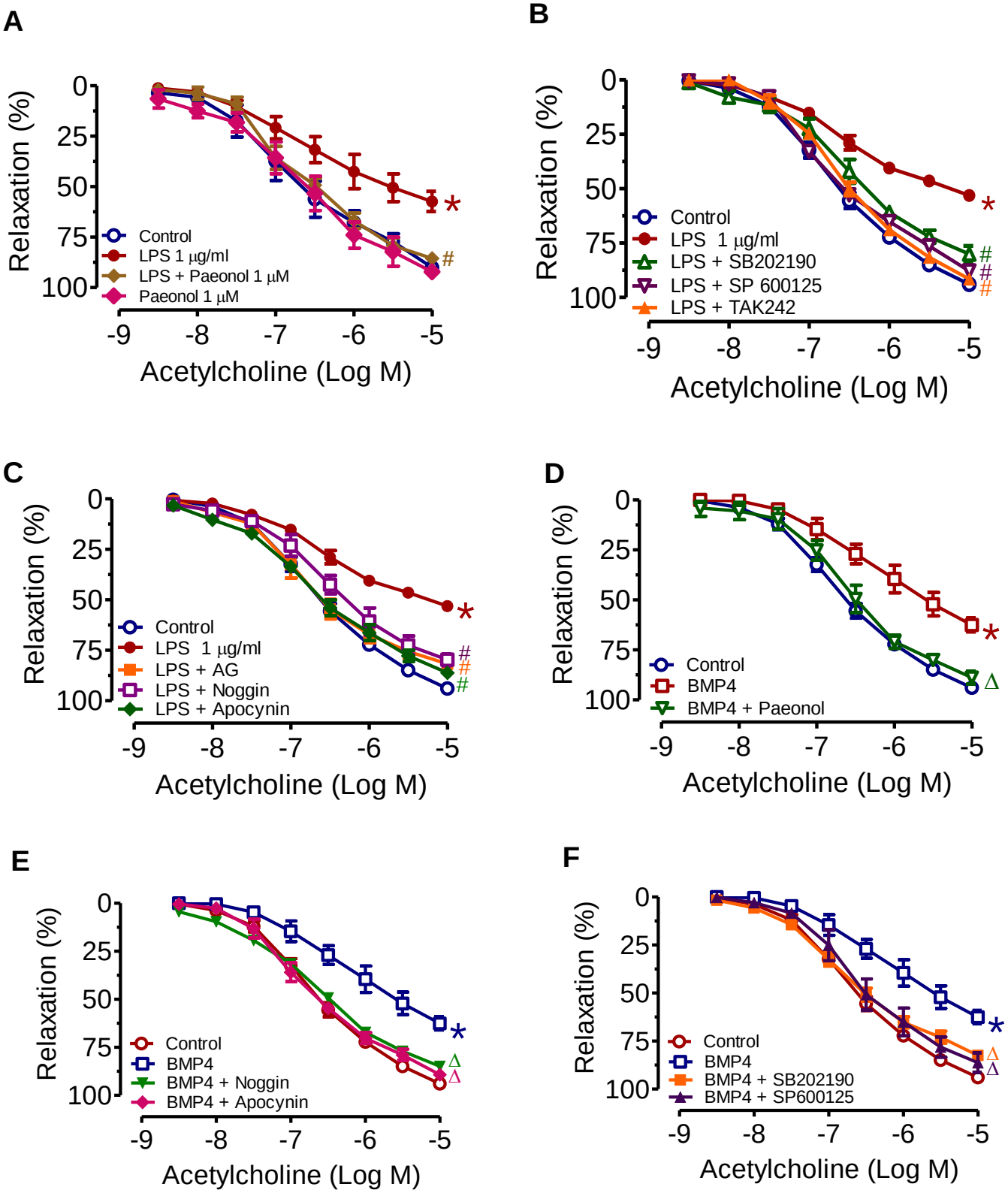
A
Relaxation (%)
0
25
50
75
100
Control
LPS 1 μg/ml
LPS + Paeonol 1 μM
Paeonol 1 μM
-9
-8
-7
-6
-5
Acetylcholine (Log M)
*
#
B
Relaxation (%)
Control
LPS 1 μg/ml
LPS + SB202190
LPS + SP 600125
LPS + TAK242
Acetylcholine (Log M)
*
#
#
#
C
Relaxation (%)
Control
LPS 1 μg/ml
LPS + AG
LPS + Noggin
LPS + Apocynin
Acetylcholine (Log M)
*
#
#
#
D
Relaxation (%)
Control
BMP4
BMP4 + Paeonol
Acetylcholine (Log M)
*
Δ
E
Relaxation (%)
Control
BMP4
BMP4 + Noggin
BMP4 + Apocynin
Acetylcholine (Log M)
*
Δ
Δ
F
Relaxation (%)
Control
BMP4
BMP4 + SB202190
BMP4 + SP600125
Acetylcholine (Log M)
*
Δ
Δ

Fig. 8

In vivo

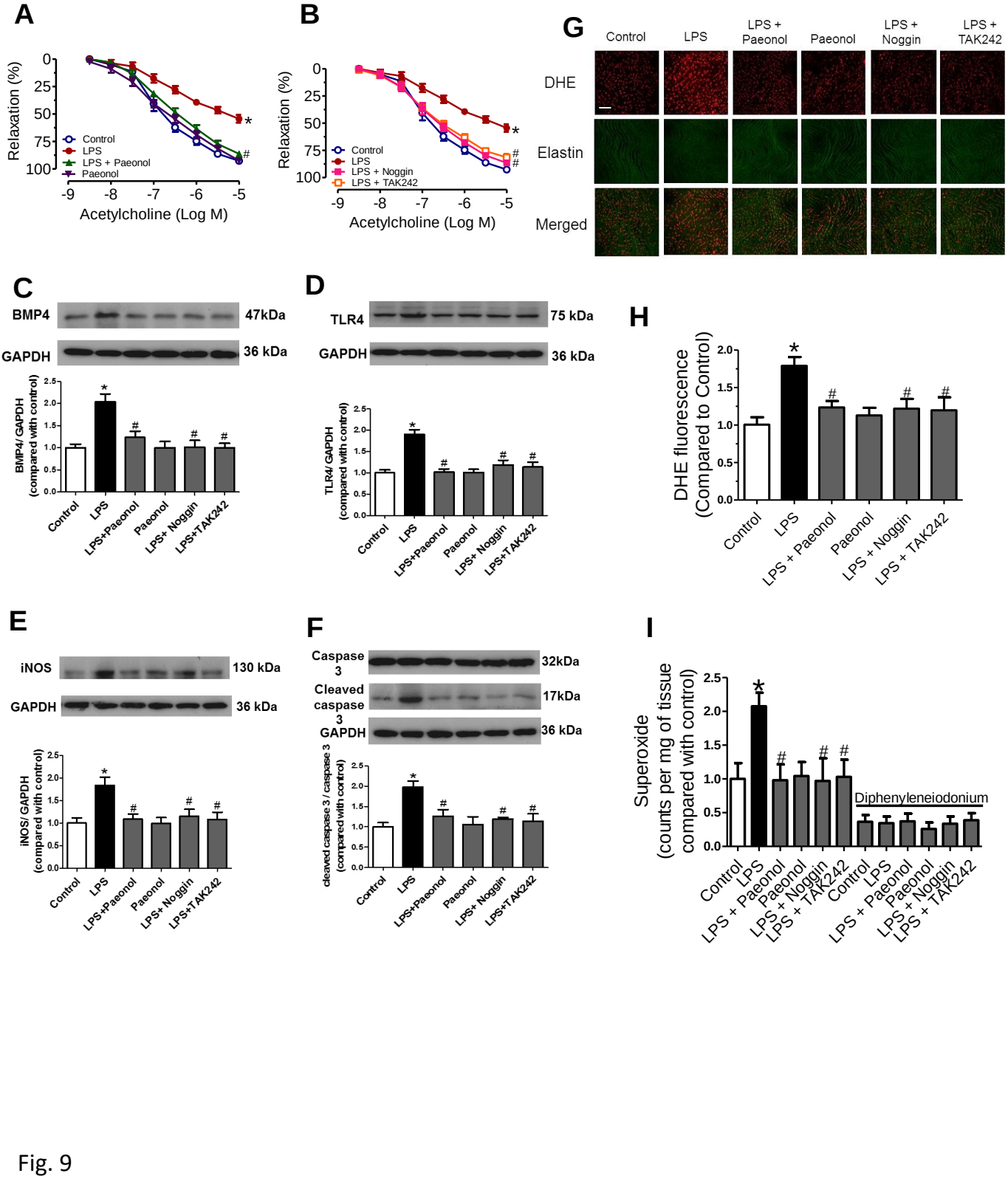
A
Relaxation (%)
0
25
50
75
100
-9
-8
-7
-6
-5
Acetylcholine (Log M)
Control
LPS
LPS + Paeonol
Paeonol
*
#
B
Relaxation (%)
Acetylcholine (Log M)
Control
LPS
LPS + Noggin
LPS + TAK242
*
#
#
G
Control
LPS
LPS + Paeonol
Paeonol
LPS + Noggin
LPS + TAK242
DHE
Elastin
Merged
C
BMP4
47kDa
GAPDH
36 kDa
BMP4/ GAPDH (compared with control)
Control
LPS
LPS+Paeonol
Paeonol
LPS+ Noggin
LPS+TAK242
D
TLR4
75 kDa
GAPDH
36 kDa
TLR4/ GAPDH (compared with control)
H
DHE fluorescence (Compared to Control)
Control
LPS
LPS + Paeonol
Paeonol
LPS + Noggin
LPS + TAK242
E
iNOS
130 kDa
GAPDH
36 kDa
iNOS/ GAPDH (compared with control)
F
Caspase 3
32kDa
Cleaved caspase 3
17kDa
GAPDH
36 kDa
cleaved caspase 3 / caspase 3 (compared with control)
I
Superoxide (counts per mg of tissue compared with control)
Diphenyleneiodonium

Fig. 9